INTERNATIONAL ATOMIC ENERGY AGENCY
UNITED NATIONS EDUCATIONAL, SCIENTIFIC AND CULTURAL ORGANIZATION
INTERNATIONAL CENTRE FOR THEORETICAL PHYSICS
I.C.T.P., P.O. BOX 586, 34100 TRIESTE, ITALY, CABLE: CENTRATOM TRIESTE

SMR.703 - 18

WORKING PARTY ON
MECHANICAL PROPERTIES OF INTERFACES

23 AUGUST - 3 SEPTEMBER 1993

"Recent Research on Mechanical Properties and the Structure of Grain Boundaries"

"Mechanical Relaxation Across Grain Boundary and the Structure of High-Angle Grain Boundaries" (Part II)

Ge Tingsui (T.S. KÊ)
Laboratory of Internal Friction and Defects in Solids
Institute of Solid State Physics
Academia Sinica
Hefei 230031
People's Republic of China

Recent Research on the Mechanical Properties and the Structure of Grain Boundaries

II. Mechanical Relaxation Across Grain Boundary and the Structure of High-Angle Grain Boundaries

Ge Tingsui (T.S. Kê)

Laboratory of Internal Friction and Defects in Solids,
Institute of Solid State Physics, Academia Sinica,
Hefei 230031, China

Abstract

Grain boundary relaxation has a profound effect on the deformation at elevated temperatures and the stress concentration as a result of the grain boundary relaxation serves as a prelude to the initiation of micro-cracks. According to the theory of linear anelasticity, the relaxation strength of grain boundary relaxation should be independent of temperature if the structure of the grain boundary does not change within the range of the temperature of measurement. If the relaxation strength does change with temperature, then we can only claim that a change of grain boundary structure has taken place giving rise to a corresponding change of the process of grain boundary relaxation.

The variation with temperature of the relaxation strength of the grain boundary relaxation in polycrystalline, bamboo-crystalline and bi-crystalline aluminium was studied with anelastic measurements. It was found that the relaxation strength decreases with lowering temperature and becomes zero at a definite temperature T_0 which is about 0.4Tm where Tm is the melting temperature of bulk aluminium. Consequently, T_0 reflects the temperature above which the grian boundary relaxation begins to be detectable. Since the boundary relaxation is closely related to the boudnary structure, so that T_0 reflects the temperature at which a structure change of the grain boundary begins to take place. The existance of such a transition tempearture T_0 conforms with the result of molecular dynamic (MD) simulation on the CSL structure as a function of tempearture. As such, we can conclude that below T_0, the boundary structure remains unchanged so that the CSL structure is maintained. However, when grian boundary relaxation takes place beginning at and above T_0, the CSL model is no longer valid and the "disordered atom group" model of high-angle boundary should be adoped for describing the mechanical properties of the grian boundary.

1. Introduction

Early in 1947, Kê demonstrated by anelastic relaxation measurements that the grain boundary in metals behaves in a viscous manner[1]. This was manifested by the appearance of an internal friction peak, the rapid drop of shear modulus, the creep under constant stress, and the stress relaxation at constant strain. Such a viscous behavior has profound effect on the deformation at elevated temperatures, and the stress concentration occurred at the grain edges and corners as a result of the stress relaxation along the boundary serves as a prelude to the initiation of micro-cracks. A through understandinng toward the relaxation parameters such as the relaxation time and the relaxation strength of grain boundary relaxation and the effect of metallurgical and structural factors on this relaxation will be very valuable in improving the mechanical properties of metals. In this connection, an elucidation of the structure of grain boundaries especially that of the high-angle boundaries is highly significant in technical as well as in academic advancement.

This paper will report the results of recent research on some fundamental aspects of grain boundary relaxation in polycrystalline, bamboo-crystalline and bi-crystalline aluminium. The variation of the relaxation strength with temperature was studied in detail. Suggestions concerning the structure of high-angle boundaries on the basis of these relaxation experiments were made.

The anelastic effects observed by Kê reflect that the grain boundary relaxation takes place under the experimental conditions at which these anelastic measurement are performed. Consider the case of internal friction, as an example. The internal friciton peak (versus temperature) and a rapid drop of shear modulus (f^2) observed by Kê in polycrystalline 99.991% aluminium which are absent in single crystal specimen are shown in Figs.1 and 2[1]. With a frequency of vibration of 0.8Hz, the internal friction begins to rise

---

Fig.1. Variation of internal friction with temperature in 99.991% polycrystalline and "single crystal" aluminium. Frequency f = 0.8Hz. [1]

Fig.2. Variation of shear modulus (f^2) with temperature in 99.991% polycrystalline and "single crystal" aluminium. [1]

---

at 200℃, reaches a maximum at 285℃ and drops afterwards. The modulus curve also begins to drop rapidly at about 200℃. This shows that the grain boundary relaxation begins to be perceptible at 200℃ when the frequency of vibration is 0.8Hz. It is to be pointed out that this commencing temperature depends on the frequency used in the measurement. Similar to other types of relaxation phenomena, the internal friciton due to grain boundary relaxation is appreciable only when the period of the applied cyclic stress is comparable to the relaxation time associated with the stress relaxation across the grian boundaries. As the rate

of grain boundary relaxation is increased by a rise of temperature, the relaxation time is reduced with an increase of temperature. Therefore when the frequency of vibration is lowered, a lower temperature is required to increase the relaxation time so that it remains comparable to the period of vibration. Accordingly the commencing temperature of detectable grain boundary relaxation is lowered when the frequency of vibration is lower. And the internal friction peak will shift to a lower temperature with a lower frequency of vibration[2]. Similarly the rapid drop of shear modulus will also commence at a lower temperature.

The height of the grain boundary internal friction peak is a measure of the relaxation strength of grain boundary relaxation. Theoretical analysis showed that the height of the internal friction peak is independent of temperature if the structure of the grain boundary does not change within the range of the temperature of measurement. Zener[3] showed that in case that the individual grains are essentially equiaxed and the grain size distribution is uniform, it is anticipated that only a fraction of the over–all stress can be relaxed by grain boundary sliding. This fraction or the relaxation strength has been shown to be dependent only on the Poisson's ratio of the specimen and is independent of temperature[3, 1]. Accordingly the height of the internal friction peak (versus temperature) which is a measure of the relaxation strength should not change when the peak was shifted toward lower temperature by using a lower frequency of vibration. Consequently if the height of the internal friction peak or the relaxation strength does change with temperature, then we can only claim that a change of grain boundary structure has taken place.

Recently, the relaxation strength associated with grian boundary relaxation in polycrystalline aluminium[4], in bamboo crystalline aluminium[5] and in aluminium bicrystals[6] has been found to decrease with temperature of measurement and becomes zero at a definite temperature T_0 which is about 0.4Tm where Tm is the melting temperature of bulk aluminium. The improtant significance of these findings is that a study on the temperature variation of grain boundary relaxation by anelastic measurements can be utilized to detect the change or the transition of the micro–structure of grain boundaries.

2. Grain Boundary Relaxation and the "Disordered Atom Group" Model of Grain Boundaries[1, 7, 4]

Consider a grain boundary with an effective thickness d. Then the coefficient of viscosity η of the grain boundary may be defined by

$$\eta = s\,(v / d), \qquad (1)$$

where s is the shearing stress and v the rate of relative displacement of the two sides of the boundary. Take the case of equiaxed grains as shown in Fig.3. Let $\triangle x$ be the distance slid

---

Fig.3. (a) Equiaxed grains. (b) Viscous sliding along grain boundary.

---

along the grain boundary during the time of relaxation τ, then

$$v \cong \triangle x / \tau. \qquad (2)$$

The shearing strain e produced by the displacement $\triangle x$ at a given temperature T is given by

$$e \cong \triangle x(T) / (GS), \qquad (3)$$

when (GS) is the average grain size. The shearing strain actually observed is

$$e = s / G(T), \qquad (4)$$

where G(T) is the shear modulus at temperature T. As these two strains must be equal, we get

$$\triangle x(T) / (GS) = s / G(T),$$

thus

$$v = \triangle x / \tau = s(GS) / G(T),$$

and

$$\eta_T = G(T)\tau d / (GS). \qquad (5)$$

The temperature dependence of τ is

$$\tau = \tau_0 exp(H / kT), \qquad (6)$$

where H is the activation energy and k the Boltzmann constant. Thus we have

$$\eta_T = \frac{G(T)\tau_0 d}{(GS)} exp(H / kT). \qquad (7)$$

Substituting into Eqn.(7) the experimental value determined by internal friction and shear modulus measurements and assuming d = 4A, the value of η is 0.18 poise at the melting point of aluminium (659.7℃). And at 670℃, it is 0.15 poise which is close to η of molten aluminium determined experimentally by Polyak and Sergee[7] having a value of 0.065 poise at 670℃.

Study on the activation energy associated with the viscous slip along grain boundaries seems to contribute to our understanding of the structure of grain boundary. It shows that the grain boundary sliding is associated with a diffusion process. Accordingly the local structure responsible for the viscous sliding along grain boudnaries must be some kind of imperfections having a local structure and can be considered as separate units. Then the regions between such "imperfection units" should be somewhat perfect and have a regular lattice structure. Thus the grain boundary structure is somewhat hetrogeneous and consists of regions of order and disorder.

A "disordered atom group" model for high-angle boundaries has been proposed by Ke[8]. The grain boundaries are assumed to be consisted of many disordered atom groups as shown schematically in Fig.4. The stress distribution around the two shaded atoms shown

---

Fig.4. Schematic illustration of a "disordered group" of atoms.

---

in the figure is different from other places, and they can pass over one another by squeezing the atoms around them. The activation energy, Hi, can be supplied by thermal agitation if the temperature is high enough. In the course of thermal agitation, the surroundings of the

two shaded atoms are subjected to a great number of rapidly varying states of stress, each representing a certain amount of energy. The number of these stress states representing an energy exceeding the value of Hi is proportional to exp(−Hi / kT). If the local state of stress changes $\mathcal{V}$ times per second, the frequency of local thermal fluctuation of energy in one direction exceeding the amount Hi is proportional to

$$\mathcal{V} \exp(-Hi / kT). \tag{8}$$

An atomic rearrangement is accomplished once the energy exceeds the value Hi, and this produces a local stress or stress release resulting in a small amount of sliding. If the atomic arrangements involve only a few atoms at a time, then it is to be expected that the activation energies for the atomic arrangement in various "disorded groups" in the grain boundary region will be densely grouped around a mean value H. The macroscopic relative displacement resulting in the atomic rearrangement in various groups are also to be expected to have a mean value.

In the absence of stress the macroscopic displacement produced in various groups are at random directions. Accordingly there is no net flow as a whole. If a shearing stress, however small, is applied as indicated in Fig.4, a preferential direction of flow is given by the directional influence of the applied stress. If the applied shear stress s is small, then the activation energy for atomic rearrangement can be expressed as $H-(1/2)V_a s$ in the direction of stress where Va is the activation volume and is independent of stress. The rate of flow along the direction of stress is, thus, proportional to

$$n\mathcal{V} \exp[(-H+\frac{1}{2}V_a s)/kT], \tag{9}$$

where n is the density of disordered groups. The activation energy in opposition to the direction of stress can be expressed as $H+(1/2)V_a s$, and the rate of flow along this direction is proportional to

$$n\mathcal{V} \exp[-H-\frac{1}{2}V_a s)/kT]. \tag{10}$$

The net rate of flow along the direction of stress is thus

$$2n\mathcal{V} \exp(-H/kT)\sinh(\frac{1}{2}V_a s/kT). \tag{11}$$

If the applied stress is small so that $(1/2)V_a s << kT$, then the rate of flow is given by

$$v = (n\mathcal{V} V_a s/kT)\exp(-H/kT), \tag{12}$$

which is proportional to the stress, and we have a Newtonian viscosity or a "pure" viscous flow. As the coefficient of viscosity is defined by $\eta = s/(v/d)$, we have

$$\eta_T = \frac{kTd}{n\mathcal{V}V_a}\exp(H/kT). \tag{13}$$

For a grain boundary having a thickness of one atomic diameter or so, we can assume that the number of "disordered atom groups" in the grain boundary region is proportional to (GS). And we can write $(1/\mathcal{V})\exp(H/kT)$ as the relaxation time τ and $(1/\mathcal{V})$ as τ_0 associated with the viscous sliding along the grain boundaries. We get finally

$$\eta_T = \frac{kT\tau_0 d}{Va(GS)} exp(H/kT). \qquad (14)$$

Comparing this expression with that derived on the basis of the viscous behavior of grain boundaries

$$\eta_T = \frac{G(T)\tau_0 d}{(GS)} exp(H/kT), \qquad (7)$$

we see that the term kT / Va in Eqn. (14) corresponds to G(T) in Eqn. (7), and both terms have the same dimensions. If the pre–experimental terms in Eqn. (14) and (7) are constant, then we have

$$\eta_T \sim \exp(H/kT),$$

and the variation of η with T should be gradual and smooth. However, as is shown in Fig.2, G(T) drops rapidly when T exceeds a certain temperature, therefore according to Eqn. (14) Va and / or τ_0 must change accordingly. An abrupt increase of Va indicate an abrupt decrease in the compactness of the atomic arrangement in the grain boundary region with the appearance of disordered atom groups. The abrupt increase of Va reduces η. Owing to the increase of Va, τ_0 will become smaller because the atoms within the disordered region are easier to rearrange and this also reduces η. This may be the reason of the rapid drop of G(T) since G(T) corresponds to kT / Va and Va plays the dominating role. It seems thus to be plausible to propose that the increase of internal friction Q^{-1} and the drop of G(T) start at a temperature at which the grian boudnary becomes disordered locally. The grain boundary relaxation (or viscous sliding) then takes place within such disordered group of atoms. We can name this temperature the transition temperature Tc of the grain boundary.

It is obvious that this transition is gradual and is effected by many metallurgical and structural factors such as impurity content, thermal and mechanical treatment on the specimen and, to be sure, on the original atomic structure of the grain boundaries as described by the model of coincidence site lattice (CSL).

3. Determination of the Commencing Temperature T_0 for Local Disordering

3.1 Polycrystalline aluminium

Now the problem is how to determine the temperature at which the local disordering should occur. According to theory of anelasticity, the position of internal friction peak and the shear modulus relaxation curve both change with the frequency of measurement. A lower frequency of vibration shifts the curves toward a lower temperature[2]. Now, if the occurrence of local disordering should depend on the frequency of vibration f, then what f should be used to determine the temperature at which local disordering occurs. As are shown in Figs.1, 2, the increase of Q^{-1} and drop of G start at about 200℃ for f = 0.8 Hz, and the largest changes occurs at 290℃. At about 350℃, Q^{-1} drops to its backgrounnd value and the change of G becomes normal. For a lower frequency of vibration, it is certain

that the increase of Q^{-1} and drop of G will start at a lower temperature. However, since Va decreases with the decrease of temperature, the sliding distance $\triangle x$ shown in Eqn. (2) becomes smaller at lower temperatures, so that the relaxation strength associated with grain boundary sliding will become smaller. As such, the height of the internal friction peak and the relaxation strength may become smaller and smaller and becomes zero eventually at sufficiently lower temperatures, then the local disordering will not occur at all. Measurements of internal friction were thus performed with 99.999% aluminium cold-drawn to 84% reduction in area and annealed at 400℃ for 1h. Internal friction curves for various frequencies of vibration are shown in Fig.5. It is seen that Q^{-1}_{max} (with internal

---

Fig.5. Variation of internal friction curves of 99.999% polycrystalline aluminium with various frequencies of vibration. Curve 1, 2, 3 for 0.1, 0.0316, 0.01 Hz respectively. The solid curves: with internal friction background subtracted.

---

friction background subtracted) is 0.086, 0.084 and 0.077 respectively when f=0.1, 0.0316 and 0.01 Hz. And the corresponding peak temperatures Tp are 260, 242 and 227℃. The half-widths of these peaks are 2.0, 2.0 and 1.9, and the β values are 2.5, 2.5 and 2.25 respectively indicating that the relaxation time has a distribution.

In this case, the internal friction can be expressed as

$$tan\varphi = \frac{J_2(x)}{J_1(x)}, \qquad x = ln\omega\tau$$

in which the compliances $J_2(x)$ and $J_1(x)$ are respectively[9]

$$J_2(x) = \delta J \cdot f_2(x, \beta)$$
$$J_1(x) = J_U + \delta J \cdot f_1(x, \beta)$$

thus

$$tan\varphi = \frac{\delta J \cdot f_2(x,\beta)}{J_U + \delta J \cdot f_1(x,\beta)}.$$

At the peak, $x = ln\omega\tau = 0$, $f_1(0, \beta) = 1/2$, we have

$$Q_m^{-1} = \frac{\delta J \cdot f_2(0,\beta)}{J_U + \delta J/2} = \frac{\triangle \cdot f_2(0,\beta)}{1 + \triangle/2}.$$

The relaxation strength $\triangle (= \delta J / J_U)$ is

$$\triangle = Q_m^{-1} / [f_2(0, \beta) - Q_m^{-1}/2], \qquad (15)$$

and the values are 0.270, 0.265, and 0.218 for three β value given above. It is seen that the relaxation strength decreases definitely at a lower Tp. However, the relaxation strength has still a definite value at 227℃.

In order to find out at what temperature the Q^{-1}_{max} and the relaxation strength will become zero, anelastic creep measurements were taken at various temperatures. In this case, we can determine the relaxation strength $\triangle(T) = (J_R - J_U)/J_U$ at temperature T, where J_U and J_R are unrelaxed and relaxed compliance respectively. Typical creep curves J(t) at

49, 83, 132, 162, 177 and 193℃ are shown in Fig.6 (curves 1 to 6). The initial compliants

Fig.6. Creep curves of 99.999% polycrystalline aluminium at various temperatures: Curves 1 to 6: At 79, 83, 132, 162, 177 and 193℃ respectively.

J(0) determined from these curves are plotted in Fig.7. It is seen that the curve J(0) vs T

Fig.7. Initial compliance J(0) of 99.999% polycrystalline aluminium at various temperatures. To indicates the temperature at which the curve starts to deviate from a straight line.

starts to deviate from a straight line at $T = T_0 = 0.42$ Tm as is marked in the figure. It has been shown[10] that if no relaxation process occurs, the curve J(0) vs T should be a straight line in a wide temperature range. Thus the deviation from straight line relationship at T_0 indicates that creep has occurred at T_0. The $\triangle(T)$ at various temperatures so determined are plotted in Fig.8 (Curve 1) and it can be seen that $\triangle(T)$ tends to become zero at

Fig.8. Variation of the relaxation strength in 99.999% polycrystalline aluminium vs temperature. Curve 1. Data from creep measurements, the vertical bars on the curve show the limits of error. Curve 2. Data from internal friction measurements.

$T = 0.43$ Tm which is very close to the value T_0 (0.42 Tm) determined in Fig.7. The $\triangle(T)$ determined by internal friction measurements are shown by curve 2 for reference. It is seen that these two curves do not coincide exactly but the tendency of change are similar.

The experimental results demonstrate that $T_0 = 0.43$ Tm so determined may be considered as the temperature at which local disordering begins in the grain boundary region in 99.999% polycrystalline aluminium. The To determined for 99.9999% aluminium is 0.35 Tm.

It has been recognized for some time that grain boundaries can undergo phase transitions similar to transformation in the bulk. Typically, Yip et la.[11, 12] by molecular dynamics simulation studies using $\sum 5 < 100 >$ symmetric tilt boundary lying parallel to {310} and pair potentials characteristic of aluminium on the structural behavior at elevated temperatures of a bicrystal of aluminium and found the bicrystal to undergo a gradual structural transition at the onset of which the grain boundary core shows significant disorder and becomes unstationary. At still higher temperature, loss of crystalline order occurs in such a decisive manner as to suggest a process of local melting. Such continuous transition begins at about 0.5 Tm with melting setting in at about 0.7 Tm.

On the contrary, calculations of grain boundary structure using pairwise atomic interaction models and the methods of molecular statics or dynamics by Balluffi et la.[13,

[4] have invariably yielded structures which may be regarded as ordered (or "crystalline") at relatively low temperatures ($<\frac{1}{2}$Tm) and can be described in terms of the structural unit model suggested by Vitek et la.[15]. Even though each type of structure unit may be distorted in various way in different parts of the core, these distortions are symmetric and periodic, and the boundary therefore exhibits a considerable degree of order. The boundary thus retains its basic crystallinity but becomes highly defective locally so that it can be described as an ordered "crystalline" structure containing high point defect concentration. Our experimental results show that the internal friction and anelastic relaxation associated with the viscous sliding along grain boundaries are attributed to the stress relaxation inside the "disordered atom groups" in grain boundary region. The temperature T_0 at which such "disordered atom group" begin to appear can be located by internal friction and micro–creep measurements. As such our experimental results do not support the proposition of local melting in the grain boundary.

3.2 Bamboo crystalline aluminium

The specimens were made of 99.999% and 99.9999% aluminium. The latter was supplied from France in the form of 1mm wire hot–extruded at 570–640 K. Metallographic examination[4]shows that grain growth has been occurred in the specimen and some of the grains have extended across the diameter of the wire. The 99.999% aluminium ingot was cut into bars with the size of $2 \times 2 \times 135$ mm and were then cold–drawn into 1 mm wire corresponding to a reduction in area of 84% reduction in area.

Three methods were used in the preparation of the bamboo–crystal specimens: (1) high temperature static annealing; (2) high temperature static annealing after previous deformation; (3) high temperature dynamic annealing after previous deformation.

Anelastic studies were made by internal friction and micro–creep measurements at various temperatures. The equipment used is a multifunction torsion apparatus designed and constructed in our own laboratory. This equipment can be used for measurements of internal friction and dynamic modulus as well as creep and stress relaxation of solid specimens at various temperature amplitudes and frequencies. Free–decay and forced–vibration measurements can be preformed with the same specimen. The equipment was controlled by an IBM–PC computer and a 8087 processor, and the data can be processed in real time. The range of frequency of vibration in forced–vibration experiments is from 10^{-5} to 10 Hz. The resolution in internal friction measurements is 1×10^{-4}.

Internal friction and shear modulus were measured in descending temperatures with a maximum strain amplitude of 1×10^{-5}. Creep measurements were taken with a step wise increase of temperature and the elastic strain used is 1×10^{-5}. The time for loading is 0.2s, after which a constant stress is maintained.

Fig.9 shows the internal friction–temperature curves of 99.999% aluminium measured

Fig.9. Variation of bamboo boundary internal friction peak with frequency in 99.999% Al

1 – ○ – 1 Hz; 2 – ◑ – 0.1 Hz; 3 – ● – 0.01 Hz

—— with internal friction background subtracted

at various frequencies by forced–vibration method. The number of bamboo boundaries contained in a specimen of 48 mm long is N = 22. Curves 1, 2 and 3 were measured at frequencies of 1, 0.1, and 0.01 Hz at descending temperatures after the specimen was annealed at 873K for 2h. The peak temperatures Tp of these curves after the subtraction of exponential high–temperature internal friction background are 478, 443 and 418K respectively. The heights of the peaks Q_m^{-1} are respectively, 0.081, 0.078 and 0.072 and the half–widths $\triangle(T^{-1})$ are, respectively 4.6×10^{-4}, 4.9×10^{-4} and 5.3×10^{-4} K^{-1}.

Curves 1, 2 and 3 in Fig.10 are the internal friction curves of 99.9999% aluminium measured at frequencies of 1, 0.1 and 0.01 Hz at descending temperatures after the specimen was annealed at 873 K for 2h. The number of bamboo boundaries contained in a specimen of 58mm long is N = 17. After the subtraction of internal friction background, Tp was found to be 412, 391 and 368 K, Q_m^{-1} to be 0.050, 0.048 and 0.042, and $\triangle(T^{-1})$ to be 5.5×10^{-4}, 5.65×10^{-4} and $6.30\times10^{-4}K^{-1}$ respectively.

It is seen from Figs.9 and 10 that the peak height Q_m^{-1} decreases with the decrease of Tp. Accordingly the relaxation strength associated with the bamboo boundary peak is a function of temperature.

Fig.10. Variation of bamboo boundary internal friction peak with frequency in 99.9999%Al

1 – ○ – 1 Hz; 2 – ● – 0.1 Hz; 3 – ◑ – 0.01 Hz

—— with internal friction background subtracted

In order to obtain a quantitative relationship between the relaxation strength and temperature, micro–creep measurements were taken on 99.9999% aluminium bamboo–crystal specimen and the creep curves measured at 288, 327, 336, 356, 366, 386 and 405 K are shown in Fig.11.

Fig.11. Creep curves of 99.9999% Al bamboo crystal specimen at various temperatures

Table 1

Relaxation strength, △, and temperature, T, in 99.9999% Al bamboo boundaries

T, K	327	336	346	356	366	386	405
$J_U(10^{-7})$	4.60	4.65	4.74	4.82	4.88	5.00	5.16
△	0.104	0.125	0.171	0,191	0.213	0.220	0.245

As has been demonstrated by theory and experiments, the elastic modulus of single crystal specimens decreases linearly with the increase of temperature if no relaxation process occurred within this temperature range [10]. Consequently if no creep occurred, then the unrelaxed compliance J_U [= J(0)] observed at various temperatures under the same applied stress should be linear with respect to temperature as shown by the straight line in Fig.12. We can thus determine the value of J_U at higher temperatures by extrapolation

Fig.12. Initial compliance J(0) of 99.9999% Al bamboo–crystal specimen at various temperatures

Tc – temperature of experimental curve starting to deviate from straight line

along the this straight line and locate the temperature at which J(t) begins to deviate from this straight line. This is the temperature at which the creep or grain boundary sliding starts to be evident. In terms of the melting temperature of bulk aluminium Tm = 933 K the value of this temperature T_0 is found from Fig.12 to be 0.35 Tm.

The relaxation strength △ at various temperatures can be evaluated according to the expression for creep $J(t) = J_U + \delta J \psi(t)$, where $\psi(t)$ is the normalized creep function. The relaxation strength △ is defined by $\triangle = \delta J / J_U$. The values of J_U and △ determined from Figs.11 and 12 are summerized in Table 1. Fig.13 shows the relationship between △ and T,

Table 2

Activation parameters of bamboo boundary relaxation in 99.9999% Al

Tp, K	$Q_m^{-1}(10^{-3})$	β	△
412	50	4.95	0.351
391	48	5.13	0.353
368	42	5.75	0.313

$H = 1.37eV; \tau_0 = 3.0 \times 10^{-15}s$

Fig.13. Variation of relaxation strength △ and temperature T for bamboo

1 – ○ – from creep measurement

2 – ● – from internal friction measurement

from which it is seen that △ decreases rapidly with the decrease of T and becomes zero at the temperature $T_0 = 0.34$ Tm. This value is identical with Tc ($= 0.35$ Tm) marked in Fig.12.

If the bamboo boundary relaxation has a single relaxation time, then the relationship between the peak height Q_m^{-1} and the relaxation strength △ should be $Q_m^{-1} = \triangle / 2$. However, this relationship does not hold as can been seen from Fig.10 and Table 2. This reflects that the relaxation time has a certain distribution. The relevant relaxation parameters, determined according to the procedure given in in Ref.[16], associated with the bamboo boundary internal friction peaks in 99.9999% Al shown in Fig.10 are summerized in Table 2.

It is seen from the table that the β value appeared in the Gauss distribution function of relaxation time varies with temperature. Linear simulation shows that β and T obey a relationship of $\beta = \mid \beta_0 - \beta_H / kT \mid$ with $\beta_0 = 1.83$, $\beta_H = 0.24$ eV. This shows that time $\tau = \tau_0 \exp(H / kT)$ both have a distribution and their variations are related to each other. The negative sign appeared in the above expression shows that the variations of $\ln\tau_0$ and H are in opposite directions. However, the H distribution plays a dominate role in the τ distribution.

In the case when the relaxation time has a distribution, the relaxation strength △ ($= \delta J / J_U$) is

$$\triangle = \frac{Q_m^{-1}}{f_2(0,\beta) - Q_m^{-1}/2}.$$

The △ values so determined are listed in Table 2 and are plotted in Fig.13 as curve 2.

Thermodynamic study of relaxation phenomena showed that the relaxation strength reflects the degree of coupling between the internal parameter ζ and the external stress. The variation of ζ is concerned with the motion of the atoms in the boundaries. As low temperatures, the boundary has a stable low-energy structure. When the temperature is elevated, the boundary structure is destroyed by thermal agitation. According to the model of coincidence site lattice, the number of coincidence sites decreases as the temperature increases, and thus leads to local disordering in the boundary region. This is just the basic idea of the model of "disordered group of atoms" [8].

Generally speaking, our results are in conformity with the atomic simulation picture of the boundary stablility reported in literatures [17, 13, 18], i.e., local disordering can occur at a relatively low temperature (~ 0.5 Tm). Our results do not support the proposition that local melting occurs at the boundary.

3.3 Aluminium Bicrystals

The raw material of 99.999% aluminium was produced in Fushun aluminium plant, China. The specimens used in the present experiments are a series of 99.999% aluminium bicrystals with [110] symmetric tilt boundary prepared by Bridgman method by Zhang Tianyi of Institute of Metal Research, Academia Sinica, Shenyang 110015, China. The raw

bicrystal is shown in Fig.14(a). A sheet specimen with a thickness of 1.2mm, a width of 4.0mm and a length of 50mm was cut along the orientation line of the raw bicrystal. After grinding and polishing treatments, it was soaked in a solution of 50% HCl + 47% HNO_3 + 3% HF for surface cleaning. The final shape of the specimen and the fashion of clamping for anelastic measurements are shown in Fig.14(b).

As can be seen from Fig.14(b), the boundary of the bicrystal is situated in the middle portion of the specimen and the boundary area is quite large ($1.2 \times 50mm^2$) along the direction of the thickness of the specimen. The clamps are gripped on the plane of the width of the specimen. During the measurements, the specimen was twisted at the upper end with the lower end fixed as shown in Fig.14(c). It is seen that the boundary is subjected to a normal stress perpendicular to the boundary plane and also a shear stress across the boundary plane. It is this shear stress that gives rise to the anelastic strain measured in the experiment.

Fig.14. (a) The as-received aluminium bicrystal. (b) The bicrystal specimen with clamp on both ends. (c) Torsional stress applied to the specimen

---

The specimen was annealed in-situ of the torsion equipment previously described at 350℃ for 2 h, and creep measurements were performed at various temperatures according to the following procedure. At each temperature, a torsional stress is applied to the specimen so that the torsion strain of the specimen reaches 2.0×10^{-5} in a time period of 0.1s. This stress σ was then maintained constant and the strain ε was measured as a function of time. Thus the torsional strain relaxation was measured under a constant torsional stress. The initial strain value of 2.0×10^{-5} was chosen to insure that the whole creep experiments were performed in an elastic (or precisely, anelastic) range. At each temperature of measurement, the compliance $J(t)$ $[=\varepsilon(t)/\sigma]$ can be computed from the corresponding σ and $\varepsilon(t)$. The time for each creep measurement is 2000s. The applied torsional stress was removed after the completion of each creep measurement at one temperature so that elastic recovery (elastic after effect) can take place in the specimen at the same temperature. After a period of time of 2000s, creep measurement was taken at a lower temperature, and so on.

Experiments have been done by cooling down the specimen to room temperature after the prior annealing at 350℃. The specimen was then heated up to successively increasing temperatures and creep measurements were performed according to similar procedure described above. The results thus obtained are the same as those obtained by successively decreasing temperatures.

A single crystal specimen was cut from the raw bicrystal [(Fig.14a)] with same dimensions as shown in Fig.14b. The conditions of this specimens are idential to the bicrystal specimen except that it does not contain any boundaries. Creep experiments with single crystal specimens did not show appreciable creep at temperatures below 210℃ or so. At temperatures higher than 210℃, some creep did occur. According to results of previous

anelastic measurements on aluminium single crystals, this creep is attributed to some high-temperature processes which occurs also in polycrystalline aluminium at high temperatures (high-temperature background) but is not connected with grian boundary process [19]. In order to avoid the effect of this high-temperature background, all creep measurements with aluminium bicrystals in the present experiment were performed at temperatures below 210℃.

As has been demonstrated by theory and experiment [11], the elastic modulus (or its reciprocal, the compliance J) of single crystal specimen decreases linearly (or the compliance J increases linearly) with the increase of temperature if no relaxation process (or creep) takes place within the same temperature range. Consequently if no creep occurs, then the unrelaxed $J_U[=J(t=0)]$ observed at various temperatures under the some applied stress should be linear with respect to temperature. This turned out to be the case for aluminium single crystals under 210℃ or so as shown in Fig.15. As J_U was determined after a loading

---

Fig.15 Unrelaxed compliance $J_U(t=0.1s)$ of 99.999% aluminium single crystal at various temperatures.

---

time of 0.1s so that it was approximated by $J(t=0.1s)$. Fig.15 shows definitely that no creep has occurred in aluminium single crystals at temperatures below 210℃.

Figure 16 shows the creep curves of an aluminium bicrystal with a misorientation angle

---

Fig.16. Creep curves of 99.999% aluminium bicrystals ($\theta=30^\circ$) at various temperatures.

$\theta = 30^\circ$ at various temperatures. The loading time for the twisting of the specimen was 0.1s. The applied torsional stress was kept constant after this time. The compliance $J(t=0.1s)$ was taken as the unrelaxed compliance J_U at the temperature concerned. Actually, the precise value of J_U should be $J(t=0)$. However, because of the limitation of the experimental conditions, precise creep measurements can only be made after a loading time of 0.1s. When the temperature is not too high, the error thus introduced is not serious.

As can be seen from the creep curves shown in Fig.16, the creep increases rapidly at first then shows down and finally approaches a saturated value which gives the value of the relaxed compliance J_R. In the case of high temperatures, the creep curve rises again after the saturated value has been reached. This exhibits the effect of the high-temperature background as has been discussed above. In such cases, the J_R was determined by drawing a horizontal line along the saturated value.

In Tab.3 are tabulated the values of J_U, J_R, $\delta J = J_R - J_U$, and the relaxation strength $\Delta = \delta J / J_U$ at various temperatures.

It can be seen from Tab.3 that in some cases, the J_U value at a lower temperature is

somewhat higher than the J_U value at an adjacent higher temperature. This is because that the loading time for the applied stress was not perfectly controlled so that the required elastic torsional strain of 2×10^{-5} was not yet reached or has been exceeded during the loading time. But such a deviation does not affect the determination of the relaxation strength $\triangle$ as $\triangle = (J_R-J_U)/J_U = J_R/J_U-1$. It can be seen that if J_U is somewhat higher than the proper value, then the whole creep curve will be elevated with a proportional increase of J_R, so that J_R/J_U and thus $\triangle$ remains unchanged at a specific temperature.

The $\triangle$ values summerized in Tab.3 were plotted against the temperature of measurement as shown in Fig.17. It is seen that $\triangle$ decreases rapidly at first and then varies

Fig.17. Variation of relaxation strength $\triangle$ with temperature for aluminium bicrystal with $\theta=30^\circ$.

according somewhat to a parabolic type. By extrapolation, $\triangle$ approaches zero at $T_o=$ 391.7K(118.5℃) or 0.42Tm whereTm=(932.85K)(659.85℃) is the melting temperature of bulk aluminium.

The variation of J_U (at $t=0.1s$) is also plotted against temperature in Fig.18. It is seen

Fig.18. Variation of $J_U(t=0.1s)$ with temperature for aluminium bicrystal with $\theta=30^\circ$.

Table 3

Relaxation parameters of aluminium bicrystal ($\theta=30^\circ$) at various temperatures.

T(℃)	$J_U\times10^7$	$J_R\times10^7$	$\delta J\times10^7$	$\triangle$
233.3	1.7377	2.2102	0.4725	0.2719
204.3	1.6546	1.9969	0.3423	0.2069
194.6	1.6142	1.9140	0.2998	0.1857
185.3	1.5784	1.8463	0.2679	0.1697
167.2	1.5038	1.7522	0.2484	0.1652
157.1	1.4731	1.6926	0.2195	0.1490
147.1	1.4387	1.5837	0.1450	0.1008
137.7	1.4357	1.5618	0.1261	0.0878
128.0	1.3847	1.4802	0.0955	0.0670
118.9	1.3367	1.4362	0.0995	0.0744

Table 4

Relaxation paramcters of aluminium by crystals ($\theta = 38.9°$) at various temperatures.

T(℃)	$J_U \times 10^8$	$J_R \times 10^8$	$\delta J \times 10^8$	△
206.8	4.1252	5.0700	0.9448	0.2290
191.3	3.8859	4.5800	0.6941	0.1786
187.7	4.1200	4.8975	0.7775	0.1887
169.1	3.7861	4.4200	0.6339	0.1674
153.2	3.6860	4.1474	0.4614	0.1252
149.5	3.6698	4.2308	0.5610	0.1529
134.3	3.5442	4.0009	0.4567	0.1289
121.9	3.6185	3.8571	0.2386	0.0659
116.0	3.5130	3.7458	0.2328	0.0663

that the temperature at which the curve begins to deviate from a linear relationship is 380.6K. If we consider this temperature to be T_o, then $T_o = 380.6K = 0.41Tm$. This is identical with the value T_o determined from the △−T curve. However, the T_o value determined from the J_U−T curve can only serve as a reference since J_U can not be measured precisely as has been discussed above.

Similar creep experiments were performed for aluminium bicrystals with $\theta = 20°$, $38.9°$, $50.5°$, $60.0°$, $70.5°$ and $153.4°$ respectively. The relaxation parameters of the bicrystals with $\theta = 38.9°$ and $50.5°$ were summerized respectively in Tabs.4 and 5 as further examples. The corresponding △−T curves and $J_U(t = 0.1s)$−T curves were plotted in Figs. 19−22 respectively. The T_o values for various θ's determined from △−T curve and J_U−T curve were summerized in Tab.6.

Table 5

Relaxation parameters of aluminium bicrystals ($\theta = 50.5°$) at various temperatures.

T(℃)	$J_U \times 10^8$	$J_R \times 10^8$	$\delta J \times 10^8$	△
206.6	6.6578	7.7250	1.0672	0.1603
202.3	4.1998	4.9127	0.7129	0.1698
192.8	4.2950	5.0233	0.7283	0.1696
173.3	3.9361	4.5600	0.6239	0.1585
163.8	3.9780	4.5750	0.5970	0.1501
144.7	3.7788	4.3400	0.5612	0.1485
125.6	3.7331	4.0400	0.3069	0.0822
115.9	3.5216	3.6586	0.1370	0.0389

Fig.19. △–T curve for $\theta = 38.9°$.

Fig.20. J_U–T curve for $\theta = 38.9°$.

Fig.21. △–T curve for $\theta = 50.5°$.

Fig.22. J_U–T curve for $\theta = 50.5°$.

Table 6

T_o for aluminium bicrystals with various θ (Tm = 932.85K)

θ	Σ	Determined from △–T curve		Determined from J_U(t = 0.1s)–T curve	
		(K)	(Tm)	(K)	(Tm)
20°		387.1	0.42	401.1	0.43
30°		391.7	0.42	380.6	0.41
38.9°	9	397.1	0.42	385.3	0.41
50.5°	11	389.7	0.42	389.7	0.42
60.0°		382.5	0.41	391.8	0.42
70.5°	3	384.2	0.41	401.2	0.43
153.4°	19a	373.1	0.40	401.1	0.43

It is seen from Tab.6 that the T_o for various θ is about 0.4 Tm which conforms with the value obtained by molecular dynamics simulation (about 0.5 Tm). This shows definitely the existence of a transformation temperature T_o at which a change of the boundary structure takes place. Such a change of boundary structure at T_o promotes the relaxation process at the boundary which can not take place or is not detectable by anelastic measurements below T_o.

It is seen that the change of T_o with θ is not evident from the results of the present experiment. Further experiments are required to make a definite conclusion.

3.4 Recent Refined Experiments with Aluminium Bicrystals (129.5°, Σ11)

In our previous creep experiment[6], a constant strain of 2×10^{-5} was set as a criterion

for the loadinng at various temperatures, and the stress necessary to give such a strain at a time period of 0.1s was maintained constant during the creep measurement. It is evident that according to this proccdure the stress applied will be different at different temperatures. This procedure is feasible if the creep strain per unit stress is independent of the applied stress. However, in order to compare the creep data at different temperatures in a rigorous way, it is desirable to take creep measurement at various temperatures under the same applied stress. This was done in the present experiment for the creep measurement of an aluminium bicrystal with misorientation angle of 129.5 ° ($\sum 11$).

The sheet bicrystal specimen was annealed in situ of the torsion equipment at 350℃ for 2h. The highest temperature for creep measurements is 206.5℃. The initial applied stress σ_0 chosen is that which gives rise to a strain of 1×10^{-5} at a time period of 0.1s. This σ_0 value was subsequently used for all creep measurements at lower temperatures. At each temperature of measurement, the compliance $J(t)[=\varepsilon(t)/\sigma_0]$ can be computed from the observed value of $\varepsilon(t)$.

It is to be pointed out that the application of stress should be instantaneous, so that $\sigma=\sigma_0$ when $t=0$ and then the unrelaxed compliance is given by $J_U=\varepsilon(0)/\sigma_0$. Since a definite time is required for the application of stress, some error will be introduced in the determination of J_U, especially at elevated temperatures. Under the present experimental conditions, a time period of 0.1s is necessary for a precise measurement of the strain ε i.e. we can only consider that $J_U=\varepsilon(t=0.1s)/\sigma_0$. The error thus introduced is not serious when the temperature of measurement is not to high.

The relaxation strength is defined by $\triangle=(J_R-J_U)/J_U=\delta J/J_0$, where J_R is the relaxed compliance and $\delta J\equiv J_R-J_U$. We have

$$J(t)=\frac{\varepsilon(t)}{\sigma_0}=J_R-(J_R-J_U)exp(-t/\tau_\sigma) \qquad (16)$$

$$=J_U+\delta J[1-exp(-t/\tau_\sigma)], \qquad (17)$$

where τ_σ is the relaxation time associated with the creep under constant applied stress. It is seen from Eq.(16) that $J_R=J(t\to\infty)$. As the creep measurement can only be proceeded to a definite period of time, an error will be introduced in the determination of J_R and thus in $\triangle$. It can be shown from Eq.(17) that

$$\frac{\triangle(t=t)}{\triangle(t\to\infty)}=1-exp(-t/\tau_\sigma),$$

and the error introduced in the determination of $\triangle$ decreases with increasing t/τ_σ. For example, the error is 5% when $t/\tau_\sigma=3$, and is 0.17% when $t/\tau_\sigma=7$.

The τ_σ at the temperature T can be valuated according to the Arrhenius relationship

$$(\tau_\sigma)_T=\tau_0 exp(H/kT),$$

where H is the activation energy and k is the Boltzmann constant. Internal friction measurement to be reported later gives

$$(\tau_\sigma)_T=3.453\times 10^{-12}exp(1.062/kT) \qquad with\ H=1.062eV.$$

The $(\tau_\sigma)_T$ at various temperatures T is given in Table 7. Taking t = 2000s as the time period for creep measurements, the $\triangle(t=2000s)/\triangle(t\to\infty)$ value is given in the last column of Table 7.

Table 7

The relaxation time $(\tau_\sigma)_T$ and $\triangle(t=2000s)/\triangle(t\to\infty)$ at various temperatures

T(℃)	$(\tau_\sigma)_T$	$\triangle(2000s)/\triangle(\infty)$
80	4947.89	0.3326
90	1892.63	0.6524
100	762.22	0.9275
110	321.89	0.9980
120	142.03	1.0000
130	65.27	1.0000
140	31.14	1.0000
150	15.39	1.0000
160	1.49	1.0000
170	0.82	1.0000
180	0.46	1.0000
190	0.26	1.0000
200	0.16	1.0000

It is seen from Table 7 that when the temperature of measurement is 100℃, the relative error introduced by evaluating J_R and $\triangle$ according to the creep measurement performed up to t = 2000s is about 7%. And this error is zero for measurements at temperatures at or higher than 110℃.

A single crystal specimen was cut from the raw bicrystal shown in Fig.23(a). Creep measurements with this specimen did not show appreciable creep at temperatures below 210℃ or so.

Fig.23 shows the creep curves at various temperatures of an aluminium bicrystal with

---

Fig.23 Creep curves measured at various temperature for 99.999 aluminium bicrystal with [110] symmetric tilt boundary (misorientation angle $\theta = 129.5°$ $\sum 11$). Curves 1–7: temperature respectively 206.5 , 196.6 , 165.6 , 145.0 , 124.6 , 104.1 , 83.9℃. Only the data up to t = 1000s are plotted in the figure

---

misorientation angle of 129.5° ($\sum 11$). The loading time for the twisting of the specimen is 0.1s. The compliance J(t = 0.1s) was taken as the unrelaxed compliance J_U at the temperature concerned. The time for each creep measurement is 2000s. It is seen from Fig.23 that the creep increases rapidly at first and then slows down and finally approaches a saturated value which gives the value of the relaxed compliance J_R. The applied torsional stress was

removed after the completion of each creep measurement at one temperature so that elastic recovery can take place in the specimen at the same temperature. After a period of time of 2000s, creep measurement was taken at a low temperature, and so on.

In Table 8 are tabulated the values of J_U, J_R, $\delta J = J_R - J_U$, and $\triangle = \delta J / J_U$ at various temperatures.

Table 8

Creep data at various temperatures for an aluminium bicrystal with misorientation angle 129.5 °

T(℃)	$J_U \times 10^8$	$J_R \times 10^8$	$\delta J \times 10^8$	$\triangle$
206.5	4.989	5.962	1.003	0.20
196.6	4.903	6.776	0.873	0.18
186.6	4.768	5.644	0.876	0.18
176.7	4.647	5.456	0.809	0.17
165.6	4.712	5.395	0.803	0.15
155.3	4.696	5.354	0.758	0.16
145.0	4.459	5.188	0.729	0.16
135.1	4.451	5.188	0.737	0.17
124.6	4.220	4.804	0.604	0.14
114.6	4.305	4.831	0.526	0.12
104.1	4.155	4.591	0.436	0.11
94.3	4.114	4.489	0.375	0.09
83.9	4.144	4.252	0.108	0.03
74.0	4.229	4.276	0.647	0.01
63.4	4.024	4.046	0.016	0.004

In Fig.24 the relaxation strength $\triangle$ is plotted against T in which it is seen that $\triangle$

Fig.24 Variation of the relaxation strength $\triangle$ with temperature for aluminium bicrystal with $\theta = 129.5°$ ($\Sigma 11$)

decreases with decreasing temperature and tends to become zero at $T_0 = 354.65K$ (81.65℃). This shows that no relaxation takes place at temperatures below this temperature T_0. Appreciable boundary relaxation begins to take place at T_0.

Creep experiments show that no relaxation takes place in single crystal specimen within the temperature range where pronounced grain boundary relaxation occurs in bicrystal. However, as has been demonstrated by theory and experiment[7], the elastic modulus (or its reciprocal, the compliance J) of single crystal specimen increases linearly (or the compliance J decreases linearly) with the decrease of temperature. Consequently if no creep associated with grain boundary relaxation occurs, then the unrelaxed $J_U[= J(t=0)]$ observed at various temperatures under the same applied stress should decrease linearly with a decrease of tem-

perature of measurement. This should be approximately true if $J_U[=J(t=0)]$ is approximated by $J_U[=J(t=0.1s)]$. For aluminium bicrystal with a misorientation angle 129.5 ° , the variation of J_U(at t = 0.1s) with temperature shown in the second column of Table 8 is plotted against the temperature in Fig.25. It is seen that the temperature at which the curve

---

Fig.25 Variation of unrelaxed compliance $J_U(t=0.1s)$ with temperature for aluminium bicrystal with $\theta = 129.5°$ (Σ11)

---

begins to deviate from a linear relationship is 371.16K (98.16℃). This shows that from this temperature upward, the creep or the grain boundary relaxation in the bicrystal specimen become pronounced so that the "J_U" observed becomes larger than the unrelaxed compliance $J_U(t=0.1s)$. Consequently, this temperature at which J_U–T curve starts to deviate from the linear relationship may be considered as the demarcation point for grain boundary relaxation. It is be pointed out that the T_0 so evaluated is only an approximate estimate since the J_U is referred to t = 0.1s instead of t = 0, so that some creep may have taken place during the time period of 0.1s.

According to the theory of anelasticity, the relaxation strength △ is given by twice of the maximum of the internal friction curve (Q^{-1}_{max}) if a single relaxation time is involved in the relaxation process. Thus the variation of relaxation strength with temperature can be evaluated from the variation of the height of the internal friction peak with temperature. The internal friction peak (versus temperature), can be shifted to lower temperature by using lower frequency of vibration. However, in case when the relaxation strength varies with temperature, the evaluation of the relaxation strength from the internal friction peak versus tmeprature will introduce intrinsic error with unreliable results.

In the present experiment, the internal friction was measured versus frequency at a constant temperature and the relaxation strength △ was evaluated from twice the maximum value of the internal friction peak versus frequency of vibration. In Fig.27(a) are shown the internal friction peaks versus frequency measured at 83.9, 104, 120, 140, 160, 180 and 200℃. The range of frequency covered is from 1×10^{-4} to 5 Hz. The strain amplitude is 1.0×10^{-5}. The corresponding internal friction peaks with the low frequency internal friction backgroup subtracted are shown in Fig.27(b). It can be seen that the peaks shift to lower frequencies and the hight of the peaks decrease with the decrease of temperature of measurement. The position and the height of the peak at various temperatures are tabulated in Table 9. The value of the relaxation time τ was evaluated by the relationship $\tau\omega = \tau 2\pi f_p = 1$ at the peak frequency.

Fig.26(a) Internal friction peaks (versus frequency) taken at various constant temperatures for aluminium bicrystal with $\theta = 129.5°$. Curves 1–7, with temperatures 200, 180, 160, 140, 120, 104 and 83.9℃ respectivelv

(b) Internal friction peaks of Fig26(a)with the low frequency internal friction background subtracted

Table 9

Position and height of the internal friction peaks (versus frequency) measured at various constant temperatures for aluminium bicrystal with $\theta = 129.5°$

T(℃)	104	120	140	160	180	200
peak frequency f_p ($Hz \times 10^3$)	0.305	1.060	3.183	19.255	70.651	192.05
$\tau(=1/2\pi f_p)$ ($s \times 10^{-3}$)	0.104	0.300	0.100	0.0165	0.00451	0.00166
peak height $_tQ^{-1}_{max}$	0.0125	0.0155	0.0175	0.0195	0.0210	0.0235

The Arrhenius plot with $\ln\tau_T$ versus $1/T$ is shown in Fig.28. From the slope of the

Fig.27 The Arrhenius plot from the data shown in Fig.26(b)

line $H/k = 1.25 \times 10^4$ we obtain $H = 1.07eV$ assuming that τ_0 in the relationship $\tau = \tau_0 \exp(H/kT)$ does not change with temperature. The result of simulation according to the method of least squares with the exponential relationship gives above is $\tau_T = 3.453 \times 10^{-12} \exp(1.062/kT)$, the value of H thus obtained (1.062eV) is very close to that obtained from the slope of the Arrhenius plot.

Assuming that the relaxation process involves a single relaxation time, then the relaxation strength $\triangle$ is given by $2Q^{-1}_{max}$. Fig.29 gives the variation of $\triangle = 2Q^{-1}_{max}$ with

Fig.28 Variation of the relaxation strength ($2Q^{-1}_{max}$) with temperature for aluminium bicrystal with $\theta = 129.5°$ ($\sum 11$)

temperature. When extropolate according to the same curvature of the curve shown in Fig.24,we got $T_0 = 348.65K$ (75.65℃).

To sum up, the T'_0s obtained by three different methods as described is 345.65, 371.15 and 348.65 K respectively and the corresponding T_0/T_m values are 0.38, 0.40 and

0.38 respectively where T_m is the melting temperature of bulk aluminium (932.85 K).

In Fig.29, the △–T curves determined by three procedures are plotted with the same

Fig.29 The relaxation strength curves measured with three methods. Curves 1–3: △–T, J_U–T, $2Q^{-1}_{max}$–T

scale. The △ value in these curves tends to become zero in the region of 0.38 to 0.40 of Tm. This shows definitely the existance of a transformation temperature T_0 for the relaxation strength of grain boundary relaxation in aluminium bicrystals.

4. Discussion and Concluding Remarks

According to the experimental results reported previously for polycrystalline[4] and bamboo crystalline[5] specimens and the present results for bicrystals, the relaxation strength of grain boundary relaxation all decreases with the decrease of temperature and becomes zero at a definite temperature T_0 which is about 0.40 of the melting temperature Tm of bulk specimen. Consequently, T_0 reflects the temperature above which the relaxation process at the boundary region begins to be detectable. Since the boundary relaxation is closely related to the boundary structure, so that T_0 reflects the temperature at which a structure change of the grain boundary begins to take place.

Recently, molecular dynamic (MD) simulation was performed on the CSL structure of [110] symmetric tilt boundary with misorientation angle 129.5° ($\sum 11$) as a function of temperature with a Morse's interaction potential. The results show that the boundary atoms begin to deviate from the CSL structure and become locally disordered in the temperature range of 300–350 K (0.32 to 0.38 Tm). This result conforms with the experimental measurements described above. As such, we can conclude that below T_0, the boundary structure remains unchanged so that the CSL structure is maintained. However, when grain boudnary relaxation takes place beginning at and above T_0, the CSL model is no longer valid, and the "disordered atom groups" model of high-angle boundary[3,4] should be adopted for describing the behavior of the grain boundary.

From the viewpoint of thermodynamics, in order that relaxation process can occur at the boundary, the Gibbs free energy $\delta G = \delta H - T\delta S$ must be $\leqslant 0$, where H is the enthalpy and S is the entropy. Thus there must be a temperature $T_0 = \delta H / \delta S$ when $\delta G = 0$, and T_0 is the commencing temperature at which the boundary structure begins to change.

References

[1] T.S.Kê, Phys. Rev. 71, 533 (1947).

[2] T.S.Kê, Phys. Rev. 72, 41 (1947).

[3] C. Zener, Phys. Rev. 60, 906 (1941).

[4] T.S.Kê, Scripta metall. meter. 24, 347 (1990).

[5] Cheng Bolin, Ge Tingsui (T.S.Kê), Acta Metallurgica Sinica, Series A, 4, 79 (1991).

[6] T.S.Kê (Ge Tingsui), Duan Yuhua, Acta metall. mater. 41, 1003 (1993).

[7] E.V. Polyak and S.V. Sergee, Comptes rendus Acad. Sci. USSR 30, 137 (1941).

[8] T.S.Kê, J. appl. Phys. 20, 274 (1949).

[9] A.S. Nowick and B.S. Berry, Anelastic Relaxation in Crystalline Solids (Academic Press, New York and London, 1972), p.96.

[10] T.S.Kê, Phys. Rev. 76, 579L (1949).

[11] P.S. Ho, T. Kwok, T. Nguyen, C. Nitta, and S. Yip, Scripta Met. 19, 993 (1985).

[12] P. Deymier, A. Taiwo and G. Kalonji, Acta metall. 35, 2719 (1987).

[13] G. Ciccotti, M. Guillope and V. Pontikisv, Phys. Rev. B27, 5576 (1983).

[14] S.W. Chan, J.S. Liu, and R.W. Balluffi, Scripta Met. 19, 1251 (1985).

[15] A.P. Sutton and V. Vitek, Phil. Trans. Roy. Soc. London A 309, 1, 37, 55 (1983).

[16] A. Seeger, M. Weller, J. Diehl, Z.L. Pan, Z.X. Zhang, and T.S.Kê, Z. Metallkunde 73, 1 (1982).

[17] R. Kikuchi, J.W. Cahn, Phys. Rev. B21, 1893 (1980).

[18] J.Q. Broughton, G.H. Gilmer, Phys. Rev. Lett. 56, 2692 (1986).

[19] T.S.Kê, J. appl. Phys. 21, 414 (1950).

CAPTION OF FIGURES

Fig.1. Variation of internal friction with temperature in 99.991% polycrystalline and "single crystal" aluminium. Frequency f ≈ 0.8Hz. [1]

Fig.2. Variation of shear modulus (f^2) with temperature in 99.991% polycrystalline and "single crystal" aluminium. [1]

Fig.3. (a) Equiaxed grains.
(b) Viscous sliding along grain boundary.

Fig.4. Schematic illustration of a "disordered group" of atoms.

Fig.5. Variation of internal friction curves of 99.999% polycrystalline aluminium with various frequencies of vibration. Curve 1, 2, 3 for 0.1, 0.0316, 0.01 Hz respectively. The solid curves: with internal friction background subtracted.

Fig.6. Creep curves of 99.999% polycrystalline aluminium at various temperatures: Curves 1 to 6: At 79, 83, 132, 162, 177 and 193℃ respectively.

Fig.7. Initial compliance J(0) of 99.999% polycrystalline aluminium at various temperatures. To indicates the temperature at which the curve starts to deviate from a straight line.

Fig.8. Variation of the relaxation strength in 99.999% polycrystalline aluminium vs temperature. Curve 1. Data from creep measurements, the vertical bars on the curve show the limits of error. Curve 2. Data from internal friction measurements.

Fig.9. Variation of bamboo boundary internal friction peak with frequency in 99.999% Al
1 – ○ – 1 Hz; 2 – ◑ – 0.1 Hz; 3 – ● – 0.01 Hz
—— with internal friction background subtracted

Fig.10. Variation of bamboo boundary internal friction peak with frequency in 99.9999% Al
1 – ○ – 1 Hz; 2 – ● – 0.1 Hz; 3 – ◑ – 0.01 Hz
—— with internal friction background subtracted

Fig.11. Creep curves of 99.9999% Al bamboo crystal specimen at various temperatures

Fig.12. Initial compliance J(0) of 99.9999% Al bamboo–crystal specimen at various temperatures
Tc – temperature of experimental curve starting to deviate from straight line

Fig.13. Variation of relaxation strength △ and temperature T for bamboo
1 – ○ – from creep measurement
2 – ● – from internal friction measurement

Fig.14. (a) The as–received aluminium bicrystal.
(b) The bicrystal specimen with clamp on both ends.
(c) Torsional stress applied to the specimen

Fig.15 Unrelaxed compliance $J_U(t=0.1s)$ of 99.999% aluminium single crystal at various temperatures.

Fig.16. Creep curves of 99.999% aluminium bicrystals ($\theta=30^\circ$) at various temperatures.

Fig.17. Variation of relaxation strength △ with temperature for aluminium bicrystal with $\theta=30^\circ$.

Fig.18. Variation of $J_U(t=0.1s)$ with temperature for aluminium bicrystal with $\theta=30^\circ$.

Fig.19. △–T curve for $\theta=38.9^\circ$.

Fig.20. J_U–T curve for $\theta=38.9^\circ$.

Fig.21. △–T curve for $\theta=50.5^\circ$.

Fig.22. J_U–T curve for $\theta = 50.5°$.

Fig.23 Creep curves measured at various temperature for 99.999 aluminium bicrystal with [110] symmetric tilt boundary (misorientation angle $\theta = 129.5°$ $\Sigma 11$). Curves 1–7: temperature respectively 206.5℃, 196.6℃, 165.6℃, 145.0℃, 124.6℃, 104.1℃, 83.9℃. Only the data up to t = 1000s are plotted in the figure

Fig.24 Variation of the relaxation strength Δ with temperature for aluminium bicrystal with $\theta = 129.5°$ ($\Sigma 11$).

Fig.25 Variation of unrelaxed compliance J_U(t = 0.1s) with temperature for aluminium bicrystal with $\theta = 129.5°$ ($\Sigma 11$).

Fig.26 (a) Internal friction peaks (versus frequency) taken at various constant temperatures for aluminium bicrystal with $\theta = 129.5°$, Curves 1–7, with temperatures 200, 180, 160, 140, 120, 104 and 83.9℃ respectively.
(b) Internal friction peaks of Fig26(a)with the low frequency internal friction background subtracted.

Fig.27 The Arrhenius plot from the data shown in Fig. 26(b).

Fig.28 Variation of the relaxation strength ($2Q^{-1}_{max}$) with temperature for aluminium bicrystal with $\theta = 129.5°$ ($\Sigma 11$).

Fig.29 The relaxation strength curves measured with three methods. Curves 1–3: Δ–T, J_U–T, $2Q^{-1}_{max}$–T.

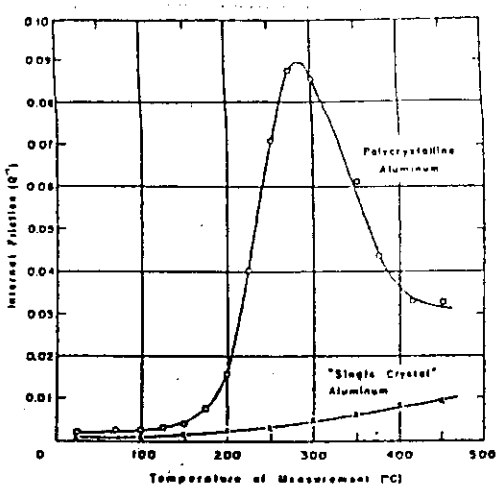

Fig.1. Variation of internal friction with temperature in 99.991% polycrystalline and "single crystal" aluminium. Frequency f = 0.8Hz. [1]

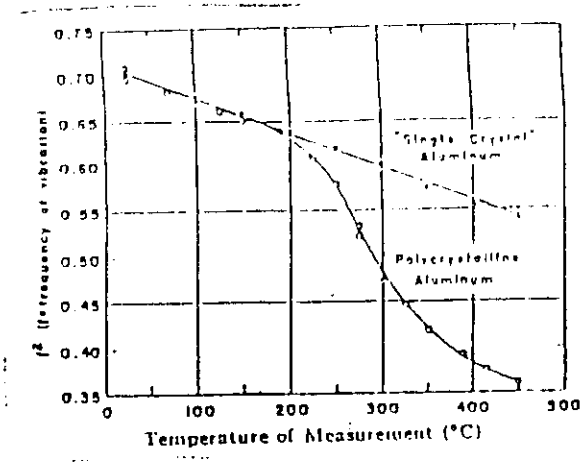

Fig.2. Variation of shear modulus (f^2) with temperature in 99.991% polycrystalline and "single crystal" aluminium. [1]

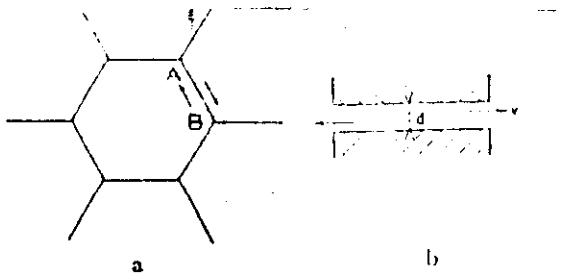

Fig.3. (a) Equiaxed grains.
(b) Viscous sliding along grain boundary.

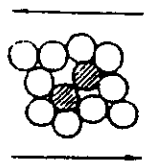

Fig.4. Schematic illustration of a "disordered group" of atoms.

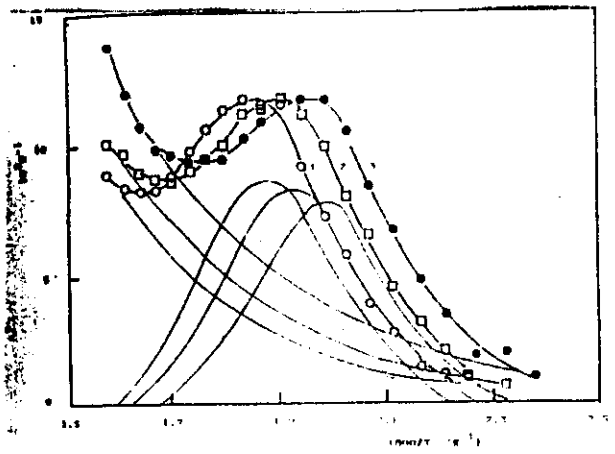

Fig.5. Variation of internal friction curves of 99.999% polycrystalline aluminium with various frequencies of vibration. Curve 1, 2, 3 for 0.1, 0.0316, 0.01 Hz respectively. The solid curves: with internal friction background subtracted.

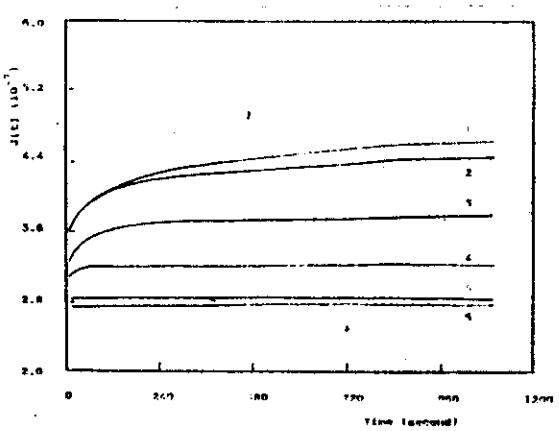

Fig.6. Creep curves of 99.999% polycrystalline aluminium at various temperatures: Curves 1 to 6: At 79, 83, 132, 162, 177 and 193°C respectively.

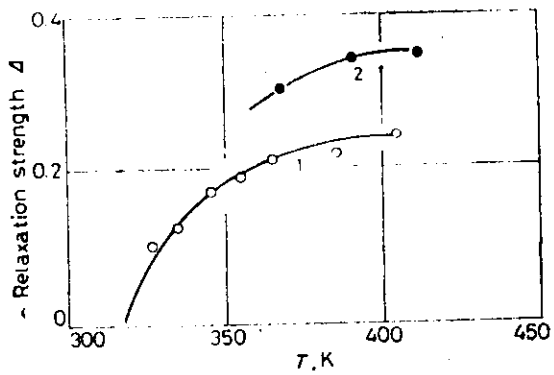

Fig.13. Variation of relaxation strength △ and temperature T for bamboo
1 – ○ – from creep measurement
2 – ● – from internal friction measurement

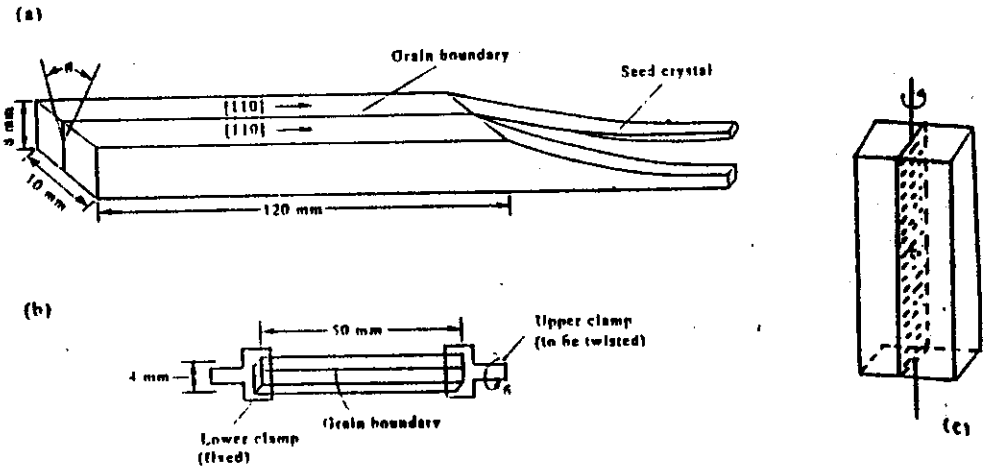

Fig.14. (a) The as-received aluminium bicrystal.
(b) The bicrystal specimen with clamp on both ends.
(c) Torsional stress applied to the specimen

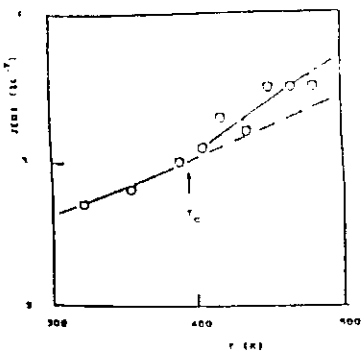

Fig.7. Initial compliance J(0) of 99.999% polycrystalline aluminium at various temperatures. Tc indicates the temperature at which the curve starts to deviate from a straight line.

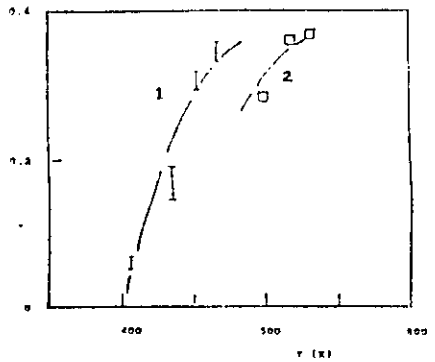

Fig.8. Variation of the relaxation strength in 99.999% polycrystalline aluminium vs temperature. Curve 1. Data from creep measurements, the vertical bars on the curve show the limits of error. Curve 2. Data from internal friction measurements.

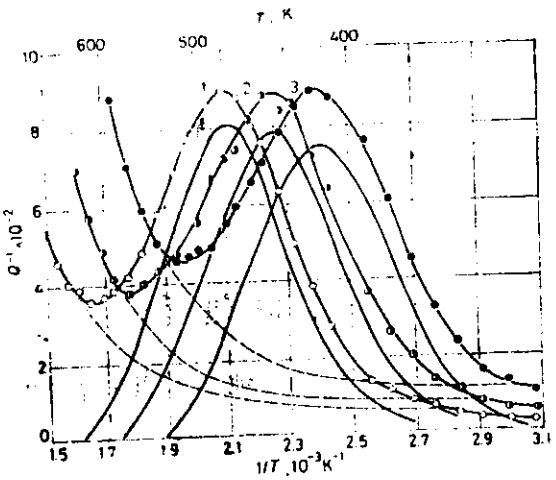

Fig.9. Variation of bamboo boundary internal friction peak with frequency in 99.999% Al
1 – ○ – 1 Hz; 2 – ◑ – 0.1 Hz; 3 – ● – 0.01 Hz
—— with internal friction background subtracted

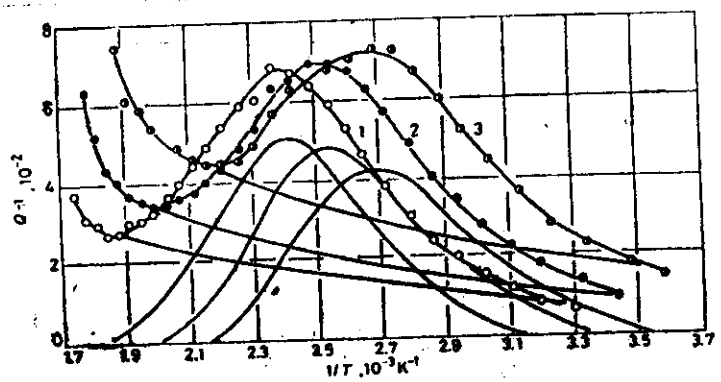

Fig.10. Variation of bamboo boundary internal friction peak with frequency in 99.9999% Al
1 – ○ – 1 Hz; 2 – ● – 0.1 Hz; 3 – ◑ – 0.01 Hz
—— with internal friction background subtracted

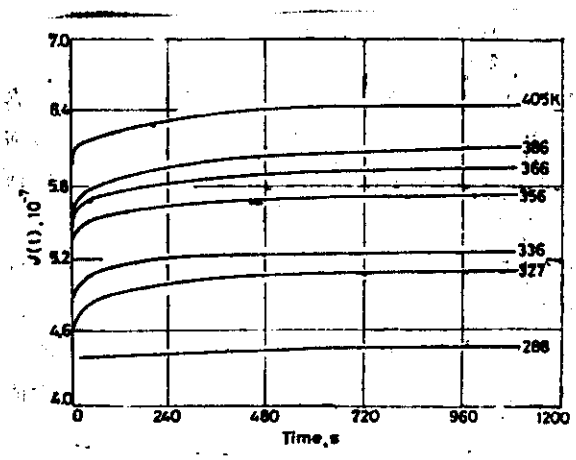

Fig.11. Creep curves of 99.9999% Al bamboo crystal specimen at various temperatures

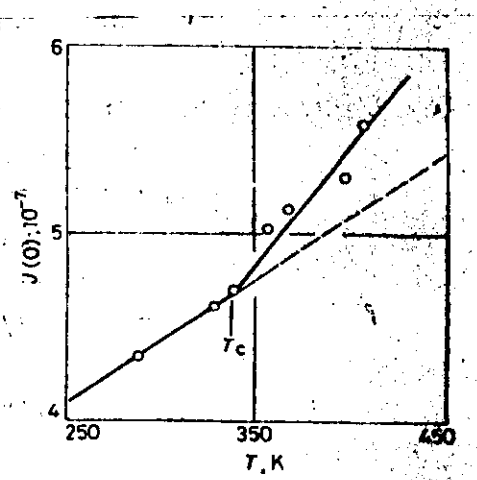

Fig.12. Initial compliance J(0) of 99.9999% Al bamboo–crystal specimen at various temperatures
Tc – temperature of experimental curve starting to deviate from straight line

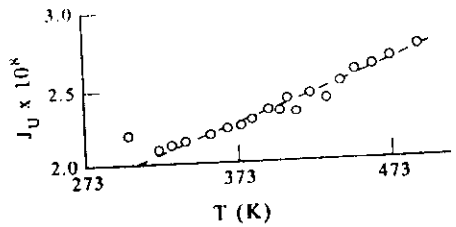

Fig.15 Unrelaxed compliance $J_U(t=0.1s)$ of 99.999% aluminium single crystal at various temperatures.

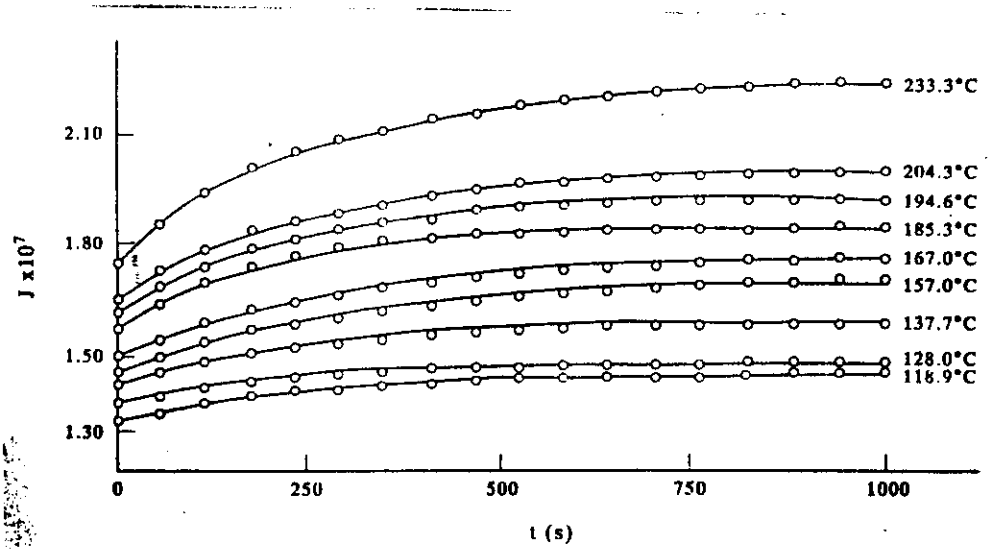

Fig.16. Creep curves of 99.999% aluminium bicrystals ($\theta = 30°$) at various temperatures.

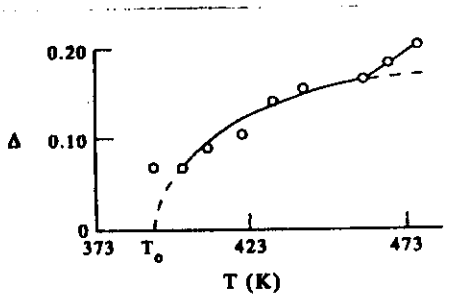

Fig.17. Variation of relaxation strength △ with temperature for aluminium bicrystal with $\theta = 30°$.

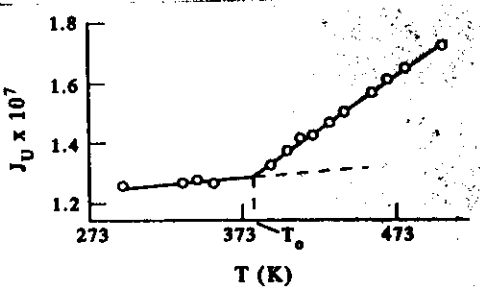

Fig.18. Variation of $J_U(t=0.1s)$ with temperature for aluminium bicrystal with $\theta = 30°$.

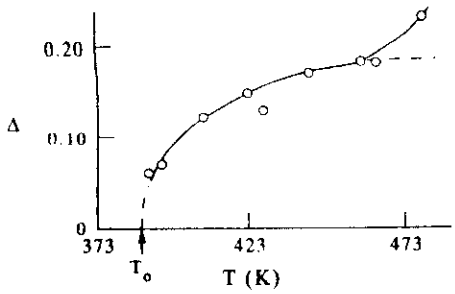

Fig.19. △–T curve for $\theta = 38.9°$.

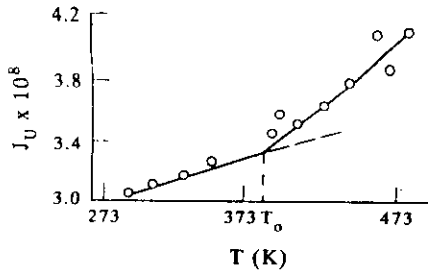

Fig.20. J_U–T curve for $\theta = 38.9°$.

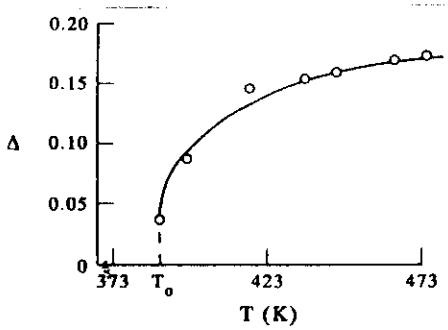

Fig.21. △–T curve for $\theta = 50.5°$.

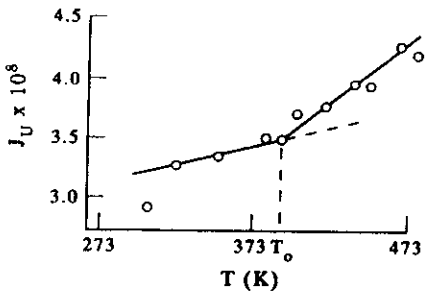

Fig.22. J_U–T curve for $\theta = 50.5°$.

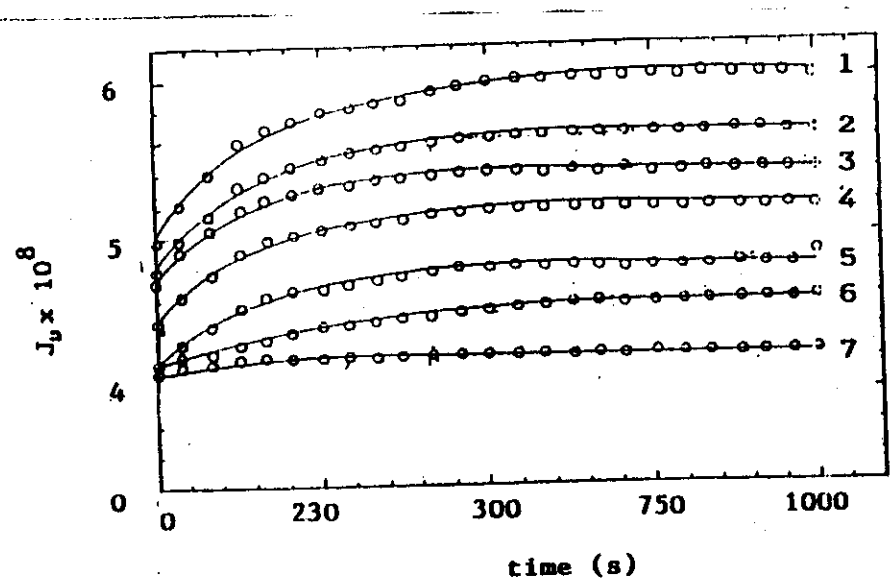

Fig.23 Creep curves measured at various temperature for 99.999 aluminium bicrystal with [110] symmetric tilt boundary (misorientation angle $\theta = 129.5° \sum 11$). Curves 1–7: temperature respectively 206.5℃, 196.6℃, 165.6℃, 145.0℃, 124.6℃, 104.1℃, 83.9℃. Only the data up to t = 1000s are plotted in the figure

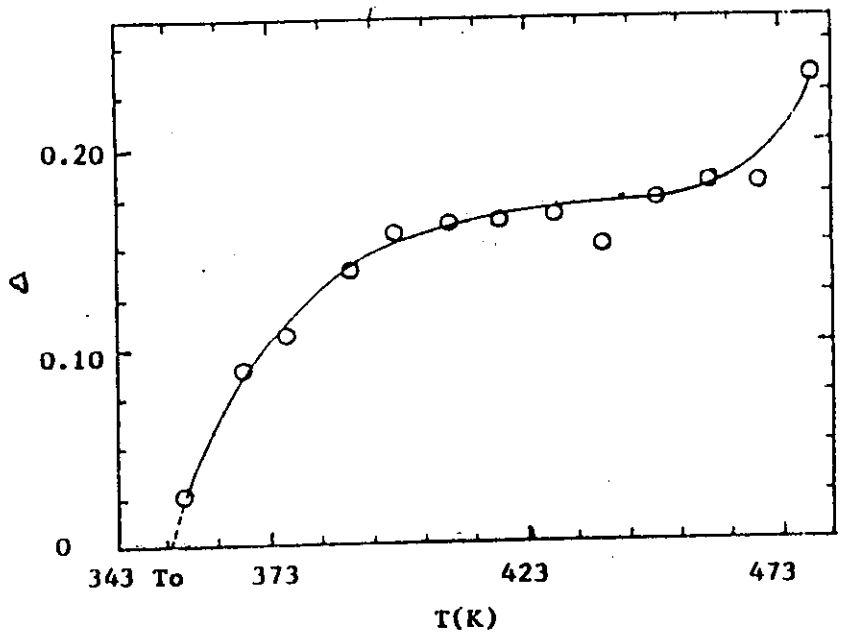

Fig.24 Variation of the relaxation strength △ with temperature for aluminium bicrystal with $\theta = 129.5^\circ$ ($\Sigma 11$).

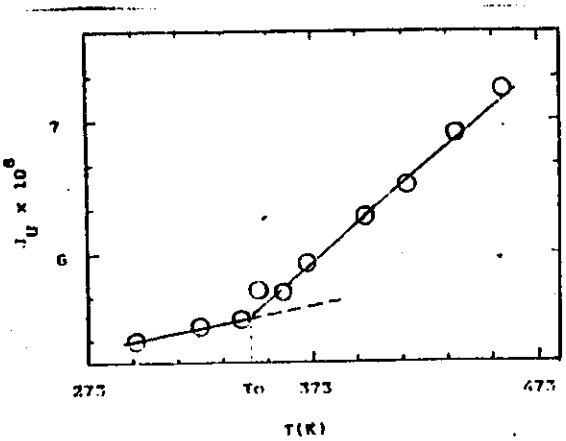

Fig.25 Variation of unrelaxed compliance $J_U(t = 0.1s)$ with temperature for aluminium bicrystal with $\theta = 129.5^\circ$ ($\Sigma 11$).

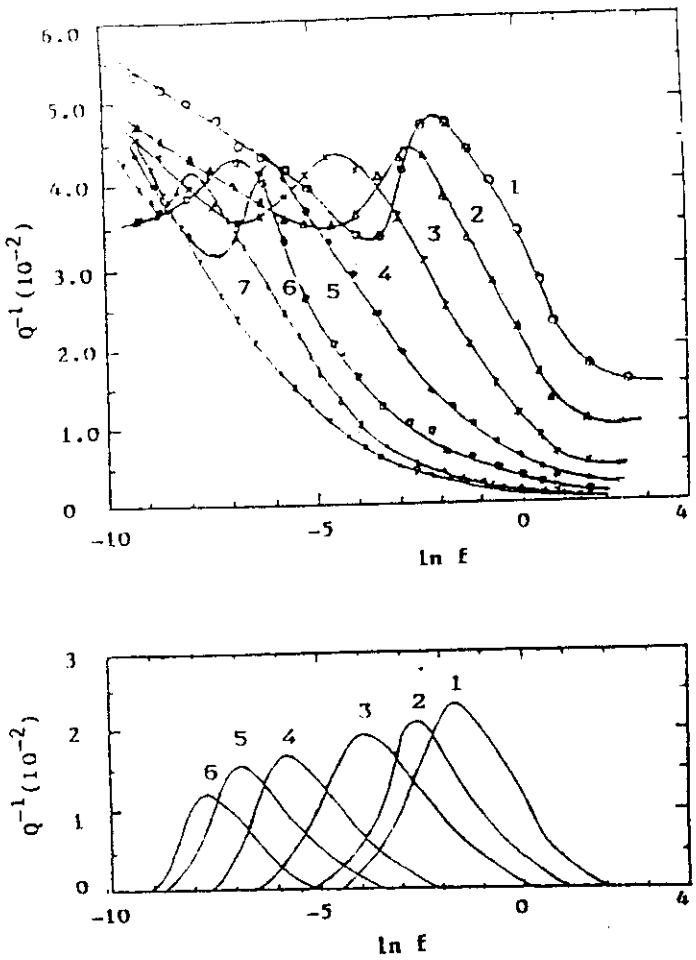

Fig.26 (a) Internal friction peaks (versus frequency) taken at various constant temperatures for aluminium bicrystal with $\theta = 129.5°$, Curves 1–7, with temperatures 200, 180, 160, 140, 120, 104 and 83.9℃ respectively. (b) Internal friction peaks of Fig.26(a) with the low frequency internal friction background subtracted.

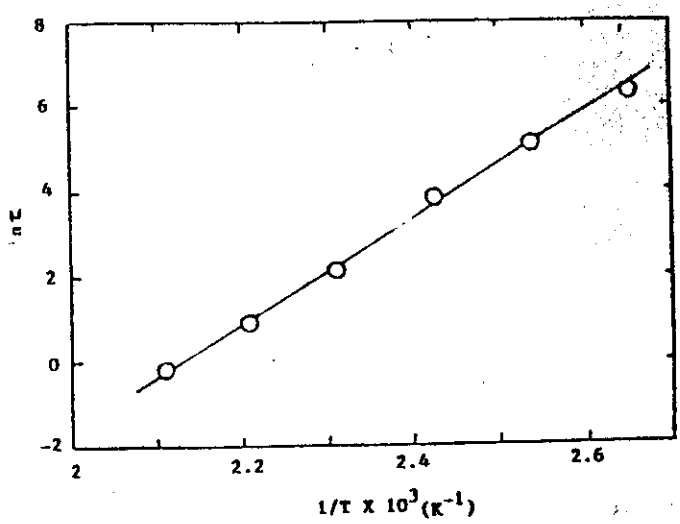

Fig.27 The Arrhenius plot from the data shown in Fig.26(b).

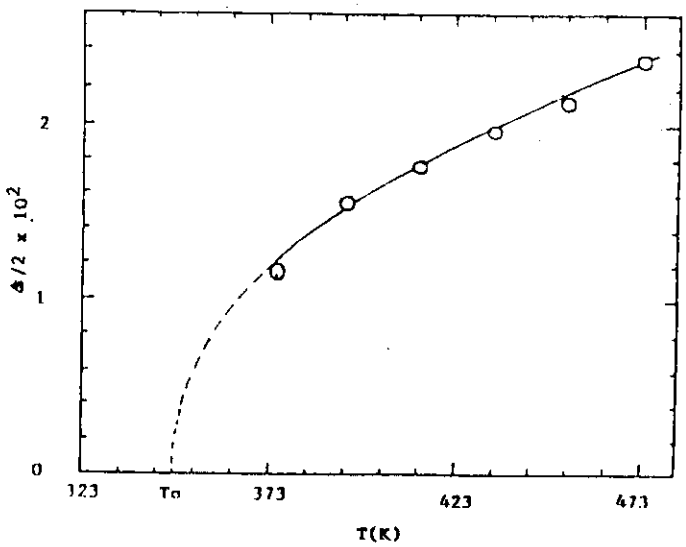

Fig.28 Variation of the relaxation strength ($2Q^{-1}_{max}$) with temperature for aluminium bicrystal with $\theta = 129.5°$ ($\Sigma 11$).

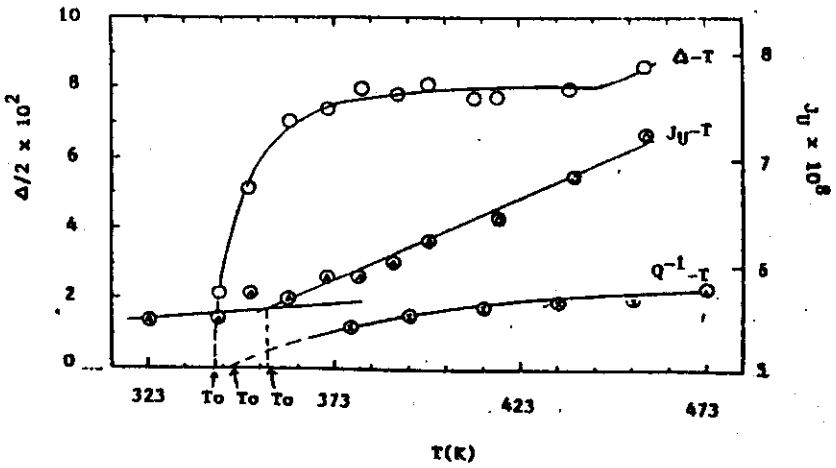

Fig.29 The relaxation strength curves measured with three methods. Curves 1–3: Δ–T, J_U–T, $2Q^{-1}_{max}$–T.